PERGAMON

International Journal of Solids and Structures 38 (2001) 1483–1494

INTERNATIONAL JOURNAL OF SOLIDS and STRUCTURES

www.elsevier.com/locate/ijsolstr

An eccentric crack in a piezoelectric strip under anti-plane shear impact loading

Jeong Woo Shin [a,1], Soon Man Kwon [a], Kang Yong Lee [b,*]

[a] *Department of Mechanical Engineering, Graduate School, Yonsei University, Seoul 120-749, South Korea*
[b] *Department of Mechanical Engineering, College of Engineering, Yonsei University, Seoul 120-749, South Korea*

Received 19 June 1999; in revised form 8 March 2000

Abstract

We consider the problem of determining the singular stress and electric fields in a piezoelectric ceramic strip containing a Griffith eccentric crack off the center line under anti-plane shear impact loading with the theory of linear piezoelectricity. Laplace transform and Fourier transforms are used to reduce the problem to a pair of dual integral equations, which are expressed to a Fredholm integral equation of the second kind. Numerical values on the dynamic stress intensity factor and the dynamic energy release rate are obtained.

Keywords: Eccentric crack; Impact loading; Field intensity factor; Energy release rate

1. Introduction

Recently, the dynamic response and the failure modes of piezoelectric materials have attracted more and more attention from many researchers. Shindo and Ozawa (1990) first investigated the steady response of a cracked piezoelectric material under the action of incident plane harmonic waves. A finite crack in an infinite piezoelectric material under anti-plane dynamic electro-mechanical impact was investigated by Chen and Yu (1997) with a well established integral transform methodology. Axisymmetric vibration of piezo-composite hollow cylinder was studied by Paul and Nelson (1996). The dynamic representation formulas and fundamental solutions for piezoelectricity were proposed by Khutoryansky and Sosa (1995). The dynamic response of a cracked dielectric medium under the action of harmonic waves in a uniform electric field was studied by Shindo et al. (1996a). In their most recent work, Narita and Shindo (1998b) investigated the scattering of Love waves by a surface-breaking crack normal to the interface in a piezoelectric layer over an elastic half plane. Li and Mataga (1996a,b) studied the semi-infinite propagating crack in a piezoelectric material with electrode boundary condition and vacuum boundary condition on the crack surface, respectively. In the work, the transient dynamic electro-mechanical loads were taken into

* Corresponding author. Fax: +82-2-361-2813.
E-mail address: fracture@yonsei.ac.kr (K.Y. Lee).
[1] Present address: Korea Aerospace Research Institute, 52 Oun-dong Yusong-gu, Taejon 306-333, South Korea.

0020-7683/01/$ - see front matter
PII: S0020-7683(00)00097-4

consideration. Shindo and Ozawa (1990) and Shindo et al. (1996b, 1997) considered the static anti-plane fracture of a cracked piezoelectric strip. Kwon and Lee (1999) obtained the solution of piezoelectric rectangular body with a center crack under anti-plane shear loading using integral transform method. Chen (1998) obtained the solution of the infinite piezoelectric strip parallel to the crack under anti-plane shear impact loading using integral transform method.

In this paper, we study the problem of a finite eccentric crack off the center line in a piezoelectric ceramic strip under anti-plane shear impact loading based on the dynamic theory of linear electroelasticity. The crack boundary condition proposed by Shindo et al. (1996b, 1997) is adopted. Laplace transform and Fourier transform are used to reduce the problem to a pair of dual integral equations, which are expressed to a Fredholm integral equation of the second kind. Numerical results for the dynamic stress intensity factor and the dynamic energy release rate are shown graphically.

2. Problem statement and method of solution

Consider a piezoelectric body in the form of an infinitely long strip containing a finite eccentric crack off the center line subjected to mechanical and electric Heaviside step pulse loadings, as shown in Fig. 1. We will consider four possible cases of boundary conditions at the edges of the strip. A set of Cartesian coordinates (x, y, z) is attached to the center of the crack. The piezoelectric ceramic strip poled with z-axis occupies the region $(-\infty < x < \infty,\ -h_2 \leqslant y \leqslant h_1,\ 2h = h_1 + h_2)$, and is thick enough in the z-direction to allow a state of anti-plane shear impact. For convenience, we assume that upper ($y \geqslant 0$, thickness h_1) and lower ($y \leqslant 0$, thickness h_2) regions of the strip cracked with the eccentricity e, off the center line, have different thickness but consist of the same material. The crack is situated along the virtual interface line $(-a \leqslant x \leqslant a,\ y = 0)$. Because of the symmetry in geometry and loading, it is sufficient to consider only the right-hand half body.

The piezoelectric boundary value problem is simplified considerably if we consider only the out-of-plane displacement and the in-plane electric fields, such that

$$u_{xi} = u_{yi} = 0, \quad u_{zi} = w_i(x, y, t), \tag{1}$$

$$E_{xi} = E_{xi}(x, y, t), \quad E_{yi} = E_{yi}(x, y, t), \quad E_{zi} = 0, \tag{2}$$

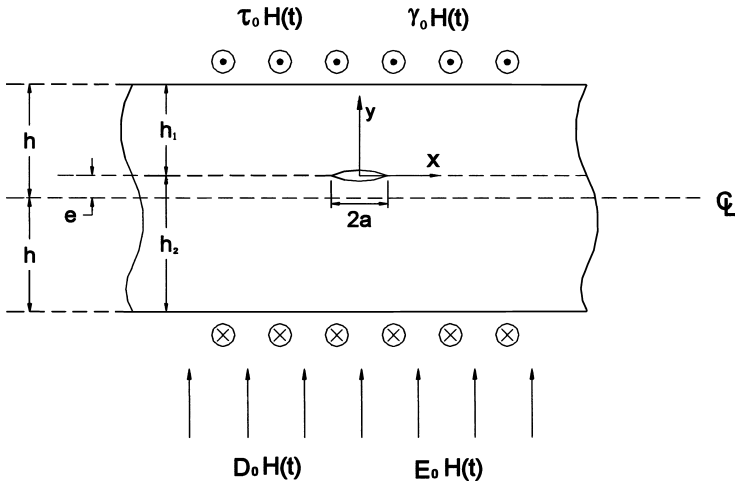

Fig. 1. A piezoelectric ceramic strip with an eccentric crack: definition of geometry and loading.

where u_{ki} and E_{ki} $(k = x, y, z)$ are displacements and electric fields, respectively. Subscript $i(i = 1, 2)$ stands for upper and lower regions, respectively.

In this case, the constitutive relations become

$$\sigma_{zji}(x, y, t) = c_{44} w_{i,j} + e_{15} \phi_{i,j}, \tag{3}$$

$$D_{ji}(x, y, t) = e_{15} w_{i,j} - d_{11} \phi_{i,j}, \tag{4}$$

where σ_{zji} and $D_{ji}(j = x, y)$ are the stress components and electric displacements, respectively. c_{44} is the elastic modulus measured in a constant electric field, d_{11} is the dielectric permittivity measured at a constant strain and e_{15} is the piezoelectric constant.

The dynamic anti-plane governing equations for piezoelectric materials are simplified to

$$c_{44} \nabla^2 w_i + e_{15} \nabla^2 \phi_i = \rho \frac{\partial^2 w_i}{\partial t^2}, \tag{5}$$

$$e_{15} \nabla^2 w_i - d_{11} \nabla^2 \phi_i = 0, \tag{6}$$

where $\nabla^2 = \partial^2/\partial x^2 + \partial^2/\partial y^2$ and ρ is a material density.

Substituting Eq. (6) into Eq. (5), we can obtain the equation of a wave motion in the form:

$$\nabla^2 w_i = \frac{1}{c_2^2} \frac{\partial^2 w_i}{\partial t^2}, \tag{7}$$

where $c_2 = \sqrt{\mu/\rho}$ and $\mu = c_{44} + e_{15}^2/d_{11}$.

The Laplace transform of Eq. (7) is in the form,

$$\nabla^2 w_i^* = \frac{p^2}{c_2^2} w_i^*, \tag{8}$$

where

$$w_i^*(x, y, p) = \int_0^\infty w_i(x, y, t) \mathrm{e}^{-pt} \, \mathrm{d}t, \tag{9}$$

$$w_i(x, y, t) = \frac{1}{2\pi i} \int_{c-i\infty}^{c+i\infty} w_i^*(x, y, p) \mathrm{e}^{pt} \, \mathrm{d}p. \tag{10}$$

The superscript $*$ stands for the Laplace transform domain.

A Fourier transform is applied to the Laplace transform of Eqs. (6) and (8), and the results are

$$w_i^*(x, y, p) = \frac{2}{\pi} \int_0^\infty [A_{1i}(s, p) \mathrm{e}^{-\gamma y} + A_{2i}(s, p) \mathrm{e}^{\gamma y}] \cos(sx) \, \mathrm{d}s + \frac{a_{0i}}{p} y, \tag{11}$$

$$\begin{aligned} \phi_i^*(x, y, p) = {} & \frac{2}{\pi} \frac{e_{15}}{d_{11}} \int_0^\infty [A_{1i}(s, p) \mathrm{e}^{-\gamma y} + A_{2i}(s, p) \mathrm{e}^{\gamma y}] \cos(sx) \, \mathrm{d}s \\ & + \frac{2}{\pi} \int_0^\infty [A_{3i}(s, p) \mathrm{e}^{-sy} + A_{4i}(s, p) \mathrm{e}^{sy}] \cos(sx) \, \mathrm{d}s - \frac{b_{0i}}{p} y, \end{aligned} \tag{12}$$

where $r = (s^2 + p^2/c_2^2)^{1/2}$ and $A_{ji}(j = 1\text{–}4)$ are the unknowns to be solved. a_{0i} and b_{0i} are real constants, which will be determined from the edge loading conditions.

Substituting Eqs. (11) and (12) into Eqs. (3) and (4) in the Laplace transform domain, we have the following:

$$\sigma^*_{yzi}(x,y,p) = \mu\frac{2}{\pi}\int_0^\infty \gamma[-A_{1i}(s,p)\mathrm{e}^{-\gamma y} + A_{2i}(s,p)\mathrm{e}^{\gamma y}]\cos(sx)\,\mathrm{d}s + e_{15}\frac{2}{\pi}\int_0^\infty s[-A_{3i}(s,p)\mathrm{e}^{-sy} + A_{4i}(s,p)\mathrm{e}^{sy}]\cos(sx)\,\mathrm{d}s + \frac{c_{0i}}{p}, \tag{13}$$

$$D^*_y(x,y,p) = -d_{11}\frac{2}{\pi}\int_0^\infty s[A_{1i}(s,p)\mathrm{e}^{-sy} + A_{2i}(s,p)\mathrm{e}^{sy}]\cos(sx)\,\mathrm{d}s + \frac{d_{0i}}{p}, \tag{14}$$

where

$$c_{0i} = c_{44}a_{0i} - e_{15}b_{0i}, \qquad d_{0i} = e_{15}a_{0i} + d_{11}b_{0i}. \tag{15}$$

The boundary conditions in the Laplace transform domain can be written as

$$\begin{cases} \sigma^*_{yzi}(x,0,p) = 0 & (0 \leqslant x < a), \\ w^*_1(x,0,p) = w^*_2(x,0,p) & (a \leqslant x < \infty), \end{cases} \tag{16}$$

$$\begin{cases} E^*_{xi}(x,0,p) = E^*_{xc}(x,0,p) & (0 \leqslant x < a), \\ \phi^*_1(x,0,p) = \phi^*_2(x,0,p) & (a \leqslant x < \infty), \end{cases} \tag{17}$$

$$\begin{cases} \sigma^*_{yz1}(x,0,p) = \sigma^*_{yz2}(x,0,p) \\ D^*_{y1}(x,0,p) = D^*_{y2}(x,0,p) & (a \leqslant x < \infty), \end{cases} \tag{18}$$

$$\text{Case 1} \quad \begin{cases} \sigma^*_{yz1}(x,h_1,p) = \sigma^*_{yz2}(x,-h_2,p) = \frac{\tau_0}{p}, \\ D^*_{y1}(x,h_1,p) = D^*_{y2}(x,-h_2,p) = \frac{D_0}{p}, \end{cases} \tag{19}$$

$$\text{Case 2} \quad \begin{cases} \gamma^*_{yz1}(x,h_1,p) = \gamma^*_{yz2}(x,-h_2,p) = \frac{\gamma_0}{p}, \\ E^*_{y1}(x,h_1,p) = E^*_{y2}(x,-h_2,p) = \frac{E_0}{p}, \end{cases} \tag{20}$$

$$\text{Case 3} \quad \begin{cases} \sigma^*_{yz1}(x,h_1,p) = \sigma^*_{yz2}(x,-h_2,p) = \frac{\tau_0}{p}, \\ E^*_{y1}(x,h_1,p) = E^*_{y2}(x,-h_2,p) = \frac{E_0}{p}, \end{cases} \tag{21}$$

$$\text{Case 4} \quad \begin{cases} \gamma^*_{yz1}(x,h_1,p) = \gamma^*_{yz2}(x,-h_2,p) = \frac{\gamma_0}{p}, \\ D^*_{y1}(x,h_1,p) = D^*_{y2}(x,-h_2,p) = \frac{D_0}{p}, \end{cases} \tag{22}$$

where the subscript c stands for the electric quantities in the crack. τ_0, D_0, γ_0 and E_0 are a uniform shear traction, electric displacement, shear strain and electric field, respectively.

By applying the edge loading conditions, the constants a_{0i} and b_{0i} as well as the unknowns in Eqs. (13) and (14) are evaluated as follows:

$$\text{Case 1} \quad a_{0i} = \frac{e_{15}D_0 + d_{11}\tau_0}{c_{44}d_{11} + e_{15}^2}, \quad b_{0i} = \frac{c_{44}D_0 - e_{15}\tau_0}{c_{44}d_{11} + e_{15}^2}, \tag{23}$$

$$\text{Case 2} \quad a_{0i} = \gamma_0, \quad b_{0i} = E_0, \tag{24}$$

$$\text{Case 3} \quad a_{0i} = \frac{\tau_0 + e_{15}E_0}{c_{44}}, \quad b_{0i} = E_0, \tag{25}$$

Case 4 $$a_{0i} = \gamma_0, \quad b_{0i} = \frac{D_0 - e_{15}\gamma_0}{d_{11}}, \tag{26}$$

$$A_{11}(s,p) = \mathrm{e}^{2\gamma h_1} A_{21}(s,p), \quad A_{12}(s,p) = \mathrm{e}^{-2\gamma h_2} A_{22}(s,p), \tag{27}$$

$$A_{31}(s,p) = \mathrm{e}^{2sh_1} A_{41}(s,p), \quad A_{32}(s,p) = \mathrm{e}^{-2sh_2} A_{42}(s,p). \tag{28}$$

The continuity condition of Eq. (18) led to the following relations between the unknowns:

$$A_{11}(s,p) - A_{12}(s,p) = A_{21}(s,p) - A_{22}(s,p), \tag{29}$$

$$A_{31}(s,p) - A_{32}(s,p) = A_{41}(s,p) - A_{42}(s,p). \tag{30}$$

It is convenient to use the following definitions:

$$A_{11}(s,p) - A_{12}(s,p) = M_A(s,p), \quad A_{31}(s,p) - A_{32}(s,p) = M_B(s,p). \tag{31}$$

Using Eqs. (27)–(31), we can obtain the following relations:

$$A_{11}(s,p) = \frac{1 - \mathrm{e}^{-2\gamma h_2}}{1 - \mathrm{e}^{-2\gamma(h_1+h_2)}} M_A(s,p), \tag{32}$$

$$A_{12}(s,p) = \frac{\mathrm{e}^{-2\gamma(h_1+h_2)} - \mathrm{e}^{-2\gamma h_2}}{1 - \mathrm{e}^{-2\gamma(h_1+h_2)}} M_A(s,p), \tag{33}$$

$$A_{21}(s,p) = \frac{\mathrm{e}^{-2\gamma h_1} - \mathrm{e}^{-2\gamma(h_1+h_2)}}{1 - \mathrm{e}^{-2\gamma(h_1+h_2)}} M_A(s,p), \tag{34}$$

$$A_{22}(s,p) = -\frac{1 - \mathrm{e}^{-2\gamma h_1}}{1 - \mathrm{e}^{-2\gamma(h_1+h_2)}} M_A(s,p), \tag{35}$$

$$A_{31}(s,p) = \frac{1 - \mathrm{e}^{-2sh_2}}{1 - \mathrm{e}^{-2s(h_1+h_2)}} M_B(s,p), \tag{36}$$

$$A_{32}(s,p) = \frac{\mathrm{e}^{-2s(h_1+h_2)} - \mathrm{e}^{-2sh_2}}{1 - \mathrm{e}^{-2s(h_1+h_2)}} M_B(s,p), \tag{37}$$

$$A_{41}(s,p) = \frac{\mathrm{e}^{-2sh_1} - \mathrm{e}^{-2s(h_1+h_2)}}{1 - \mathrm{e}^{-2s(h_1+h_2)}} M_B(s,p), \tag{38}$$

$$A_{42}(s,p) = -\frac{1 - \mathrm{e}^{-2sh_1}}{1 - \mathrm{e}^{-2s(h_1+h_2)}} M_B(s,p). \tag{39}$$

The electric potential in the crack can be derived in the form,

$$\phi_{\mathrm{c}}^*(x,y) = \frac{2}{\pi} \int_0^\infty C(s,p) \sinh(sy) \cos(sx)\, \mathrm{d}s \quad (0 \leqslant x < a), \tag{40}$$

where $C(s,p)$ is also unknown. Using Eq. (40) and the mixed boundary condition Eq. (17), we obtained the following dual integral equations:

$$\int_0^\infty s[e_{15}F(s,p)M_A(s,p)+d_{11}G(s)M_B(s,p)]\sin(sx)\,\mathrm{d}s=0 \quad (0\leqslant x<a),$$
$$\int_0^\infty M_B(s,p)\cos(sx)\,\mathrm{d}s=0 \quad (a\leqslant x<\infty), \tag{41}$$

where

$$F(s,p)=\frac{(1+\mathrm{e}^{-2\gamma h_1})(1-\mathrm{e}^{-2\gamma h_2})}{1-\mathrm{e}^{-2\gamma(h_1+h_2)}}=\frac{2\tanh(\gamma h_2)}{\tanh(\gamma h_1)+\tanh(\gamma h_2)}, \tag{42}$$

$$G(s)=\frac{(1+\mathrm{e}^{-2sh_1})(1-\mathrm{e}^{-2sh_2})}{1-\mathrm{e}^{-2s(h_1+h_2)}}=\frac{2\tanh(sh_2)}{\tanh(sh_1)+\tanh(sh_2)}. \tag{43}$$

Using Eq. (41) and the mixed boundary condition (16), we obtain the following dual integral equations:

$$\int_0^\infty s[f(s,p)M_A(s,p)]\cos(sx)\,\mathrm{d}s=\frac{\pi}{2}\frac{c_0}{p} \quad (0\leqslant x<a),$$
$$\int_0^\infty M_A(s,p)\cos(sx)\,\mathrm{d}s=0 \quad (a\leqslant x<\infty), \tag{44}$$

where

$$f(s,p)=\frac{1}{c_{44}}\left[\frac{1-\mathrm{e}^{-2\gamma h_2}}{1-\mathrm{e}^{-2\gamma(h_1+h_2)}}\right]\left[\frac{\mu\gamma}{s}(1-\mathrm{e}^{-2\gamma h_1})-\frac{e_{15}^2}{d_{11}}\left(\frac{1-\mathrm{e}^{-2sh_1}}{1+\mathrm{e}^{-2sh_1}}\right)(1+\mathrm{e}^{-2\gamma h_1})\right]$$
$$=\frac{1}{c_{44}}\frac{2\tanh(\gamma h_2)}{\tanh(\gamma h_1)+\tanh(\gamma h_2)}\left[\mu\frac{\gamma}{s}\tanh(\gamma h_1)-\frac{e_{15}^2}{d_{11}}\tanh(sh_1)\right], \tag{45}$$

$$c_0=c_0^{(1)}=c_0^{(2)}. \tag{46}$$

Eq. (44) may be solved by using new function $\Phi_*^1(\xi,p)$ defined by

$$M_A(s,p)=\int_0^a \xi\Phi_1^*(\xi,p)J_0(s\xi)\,\mathrm{d}\xi, \tag{47}$$

where $J_0(\ )$ is the zero-order Bessel function of the first kind.

Inserting Eq. (47) into Eq. (44), we can find that the auxiliary function $\Phi_1^*(\xi,p)$ is given by a Fredholm integral equation of the second kind in the form,

$$\Phi_1^*(\xi,p)+\int_0^a K(\xi,\eta,p)\Phi_1^*(\eta,p)\,\mathrm{d}\eta=\frac{\pi}{2}\frac{c_0}{p}, \tag{48}$$

where

$$K(\xi,\eta,p)=\eta\int_0^\infty s\{f(s,p)-1\}J_0(s\eta)J_0(s\xi)\,\mathrm{d}s. \tag{49}$$

We introduce the following dimensionless variables and functions for numerical analysis:

$$s=S/a,\quad \eta=aH,\quad \xi=a\Xi,\quad \gamma=\Gamma/a,$$
$$\Phi_1^*(\xi,p)=\frac{\pi}{2}\frac{c_0}{p}\frac{\Psi_1^*(\Xi,p)}{\sqrt{\Xi}},\quad \Phi_1^*(\eta,p)=\frac{\pi}{2}\frac{c_0}{p}\frac{\Psi_1^*(H,p)}{\sqrt{H}}. \tag{50}$$

Substituting Eq. (50) into Eqs. (48) and (49), the following Fredholm integral equation of the second kind is obtained:

$$\Psi_1^*(\Xi,p)+\int_0^1 L(\Xi,H,p)\Psi_1^*(H,p)\,\mathrm{d}H=\sqrt{\Xi}, \tag{51}$$

where

$$L(\Xi,H,p)=\sqrt{\Xi H}\int_0^\infty S\left\{f\left(\frac{S}{a},p\right)-1\right\}J_0(SH)J_0(S\Xi)\,\mathrm{d}S, \tag{52}$$

$$f\left(\frac{S}{a},p\right)=\frac{1}{c_{44}}\frac{2\tanh\left(\Gamma\frac{h_2}{a}\right)}{\tanh\left(\Gamma\frac{h_1}{a}\right)+\tanh\left(\Gamma\frac{h_2}{a}\right)}\left[\mu\frac{\Gamma}{S}\tanh\left(\Gamma\frac{h_1}{a}\right)-\frac{e_{15}^2}{d_{11}}\tanh\left(S\frac{h_1}{a}\right)\right], \tag{53}$$

$$h_1=h-e,\quad h_2=h+e. \tag{54}$$

3. Field intensity factors and energy release rate

The mode III stress intensity factor in the Laplace transform domain, $K_{\mathrm{III}}^*(p)$, is determined by the following formula:

$$K_{\mathrm{III}}^*(p)\equiv\lim_{x\to a^+}\sqrt{2\pi(x-a)}\sigma_{yzi}^*(x,0,p)=\frac{c_0}{p}\sqrt{\pi a}\Psi_1^*(1,p). \tag{55}$$

From the inverse Laplace transform of Eq. (55), we obtain the dynamic intensity factor in the physical space in the form,

$$K_{\mathrm{III}}=c_0\sqrt{\pi a}M(t), \tag{56}$$

where

$$M(t)=\frac{1}{2\pi i}\int_{c-i\infty}^{c+i\infty}\frac{\Psi_1^*(1,p)}{p}\mathrm{e}^{pt}\,\mathrm{d}p, \tag{57}$$

and the function $\Psi_1^*(1,p)$ is obtained from Eq. (51).

Extending the traditional concept of stress intensity factor to other field variables, we have

$$\gamma_{xz}=-\frac{K^{\mathrm{S}}}{\sqrt{2\pi r}}\sin\left(\frac{\theta}{2}\right),\qquad \gamma_{yz}=\frac{K^{\mathrm{S}}}{\sqrt{2\pi r}}\cos\left(\frac{\theta}{2}\right), \tag{58}$$

$$E_x=-\frac{K^{\mathrm{E}}}{\sqrt{2\pi r}}\sin\left(\frac{\theta}{2}\right),\qquad E_y=\frac{K^{\mathrm{E}}}{\sqrt{2\pi r}}\cos\left(\frac{\theta}{2}\right), \tag{59}$$

$$\sigma_{xz}=-\frac{K^{\mathrm{T}}}{\sqrt{2\pi r}}\sin\left(\frac{\theta}{2}\right),\qquad \sigma_{yz}=\frac{K^{\mathrm{T}}}{\sqrt{2\pi r}}\cos\left(\frac{\theta}{2}\right), \tag{60}$$

$$D_x=-\frac{K^{\mathrm{D}}}{\sqrt{2\pi r}}\sin\left(\frac{\theta}{2}\right),\qquad D_y=\frac{K^{\mathrm{D}}}{\sqrt{2\pi r}}\cos\left(\frac{\theta}{2}\right), \tag{61}$$

where K^{S}, K^{E}, K^{T} and K^{D} are the dynamic strain intensity, electric field intensity, stress intensity and electric displacement intensity factor, respectively. These field intensity factors can be obtained as follows:

$$K^{\mathrm{S}}=\frac{K_{\mathrm{III}}}{c_{44}}=\frac{c_0}{c_{44}}\sqrt{\pi a}M(t), \tag{62}$$

$$K^{\mathrm{E}}=0, \tag{63}$$

$$K^{\mathrm{T}} = K_{\mathrm{III}} = c_0\sqrt{\pi a}M(t), \tag{64}$$

$$K^{\mathrm{D}} = \frac{e_{15}}{c_{44}}K_{\mathrm{III}} = \frac{e_{15}c_0}{c_{44}}\sqrt{\pi a}M(t), \tag{65}$$

Evaluating the energy release rate J for the anti-plane case obtained by Narita and Shindo (1998a) on a vanishingly small contour at a crack tip, we obtain

$$J = \frac{K^{\mathrm{T}}K^{\mathrm{S}}}{2} = \frac{K_{\mathrm{III}}^2}{2c_{44}} = \frac{\pi a}{2c_{44}}c_0^2[M(t)]^2. \tag{66}$$

4. Discussion

4.1. Case study

(1) The expressions of a dynamic energy release rate for the four possible boundary conditions are obtained in the forms:

$$\text{Case 1} \quad J = \tfrac{\pi a}{2c_{44}}\tau_0^2[M(t)]^2, \tag{67}$$

$$\text{Case 2} \quad J = \tfrac{\pi a}{2c_{44}}[c_{44}\gamma_0 - e_{15}E_0]^2[M(t)]^2, \tag{68}$$

$$\text{Case 3} \quad J = \tfrac{\pi a}{2c_{44}}\tau_0^2[M(t)]^2, \tag{69}$$

$$\text{Case 4} \quad J = \tfrac{\pi a}{2c_{44}}\left[\tfrac{(c_{44}d_{11}+e_{15}^2)\gamma_0 - e_{15}D_0}{d_{11}}\right]^2[M(t)]^2. \tag{70}$$

From Eqs. (67)–(70), the dynamic energy release rates are dependent on the electric loading only under constant strain loading and independent of it under constant stress loading and always have positive values.

(2) Since $\Psi_1^*(1,p) = 1$ and $M(t) = H(t)$ in Eqs. (51)–(53) and Eq. (57) as $h_1, h_2 \to \infty$, the dynamic energy release rate J_∞ for an infinite piezoelectric ceramic can be obtained from Eq. (66) in the form:

$$J_\infty = \frac{\pi a}{2c_{44}}c_0^2[H(t)]^2. \tag{71}$$

(3) The static solution of this problem can be derived from Eq. (51) by Tauberian theorem (Sneddon, 1972).

$$\Psi_1(\Xi) + \int_0^1 L(\Xi H)\Psi_1(H)\,\mathrm{d}H = \sqrt{\Xi}, \tag{72}$$

$$L(\Xi, H) = \sqrt{\Xi H}\int_0^\infty S\{f(S/a) - 1\}J_0(SH)J_0(S\Xi)\,\mathrm{d}S, \tag{73}$$

$$f\left(\frac{S}{a}\right) = \frac{2\tanh(\frac{S}{a}h_1)\tanh(\frac{S}{a}h_2)}{\tanh(\frac{S}{a}h_1) + \tanh(\frac{S}{a}h_2)} = \tanh\left(\frac{h}{a}S\right) - \frac{2\sinh^2(\frac{e}{a}S)}{\sinh(2\frac{h}{a}S)}. \tag{74}$$

(4) Since $h_1 = h_2 = h$ as $e \to 0$, we can find the solution for an infinite strip parallel to the center crack as follows:

$$L(\Xi,H,p)=\sqrt{\Xi H}\int_0^\infty S\left\{f\left(\frac{S}{a},p\right)-1\right\}J_0(SH)J_0(S\Xi)\,\mathrm{d}S, \tag{75}$$

$$f\left(\frac{S}{a},p\right)=\frac{1}{c_{44}}\left[\mu\frac{\Gamma}{S}\tanh\left(\Gamma\frac{h}{a}\right)-\frac{e_{15}^2}{d_{11}}\tanh\left(\frac{S}{a}\right)\right]. \tag{76}$$

(5) In the case of $h_2\to\infty$ and $h_1=h$, we find the kernel function $L(\Xi,H,p)$ in the form,

$$L(\Xi,H,p)=\sqrt{\Xi H}\int_0^\infty S\left\{f\left(\frac{S}{a},p\right)-1\right\}J_0(SH)J_0(S\Xi)\,\mathrm{d}S, \tag{77}$$

$$f\left(\frac{S}{a},p\right)=\frac{1}{c_{44}}\frac{2}{1+\tanh\left(\Gamma\frac{h}{a}\right)}\left[\mu\frac{\Gamma}{S}\tanh\left(\Gamma\frac{h}{a}\right)-\frac{e_{15}^2}{d_{11}}\tanh\left(S\frac{h}{a}\right)\right]. \tag{78}$$

4.2. Effects of eccentricity and crack length

The dynamic stress intensity factor and the dynamic energy release rate, Eq. (51) is computed numerically by Gaussian quadrature formulas. The inverse Laplace transformations of the intensity factors are carried out by the numerical method described by Miller and Guy (1966). We consider PZT-5H piezoceramic, and the material properties as follows (Pak, 1990):

$$c_{44}=3.53\times10^{10}\ (\mathrm{N/m^2}),\quad e_{15}=17.0\ (\mathrm{C/m^2}),\quad d_{11}=151\times10^{-10}\ (\mathrm{C/V\,m}),$$

where N, C, and V are the force in Newtons, charge in coulombs and the electric potential in volts, respectively.

Figs. 2 and 3 display the variations of the normalized dynamic stress intensity factor $K_{\mathrm{III}}/c_0\sqrt{\pi a}$ and the normalized dynamic energy release rate J/J_∞ against c_2t/a with various a/h values at $e/h=0$. The normalized dynamic stress intensity factor and the normalized dynamic energy release rate rise rapidly with

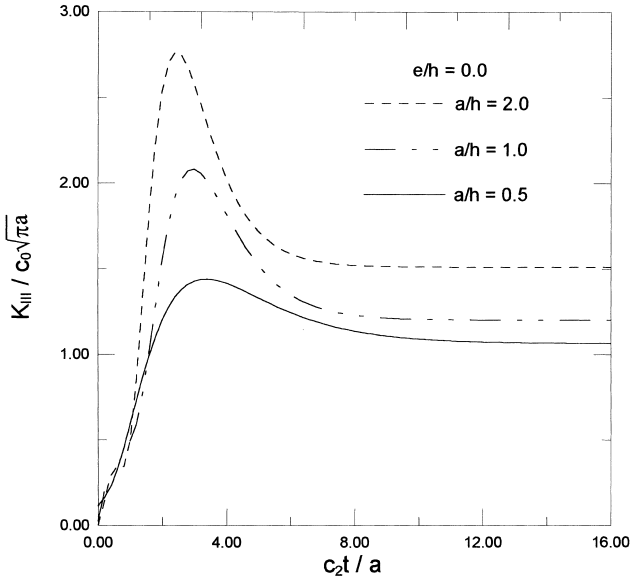

Fig. 2. Dynamic stress intensity factor $K_{\mathrm{III}}/c_0\sqrt{\pi a}$ of PZT-5H for various a/h values.

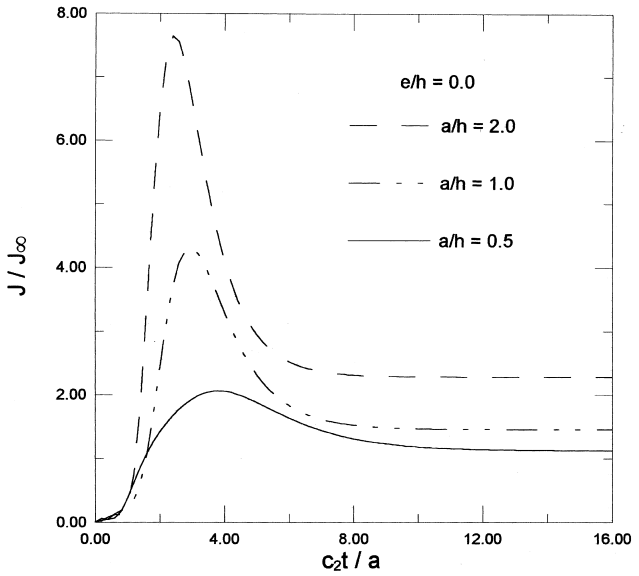

Fig. 3. Dynamic energy release rate of PZT-5H for various a/h values.

time, reaching a peak, then decrease in magnitude to reach static values. Peak values increase as a/h increases. The larger the length a/h, the faster the time in arriving at peak values.

Figs. 4 and 5 show the variations of the normalized dynamic stress intensity factor and the normalized dynamic energy release rate against c_2t/a with various e/h values at $a/h = 1.0$. In this case, the trends with time are similar to those of Figs. 2 and 3.

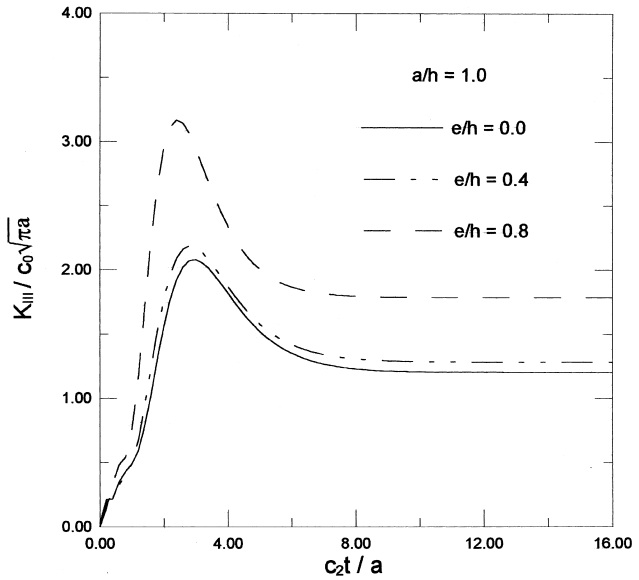

Fig. 4. Dynamic stress intensity factor $K_{III}/c_0\sqrt{\pi a}$ of PZT-5H for various e/h values.

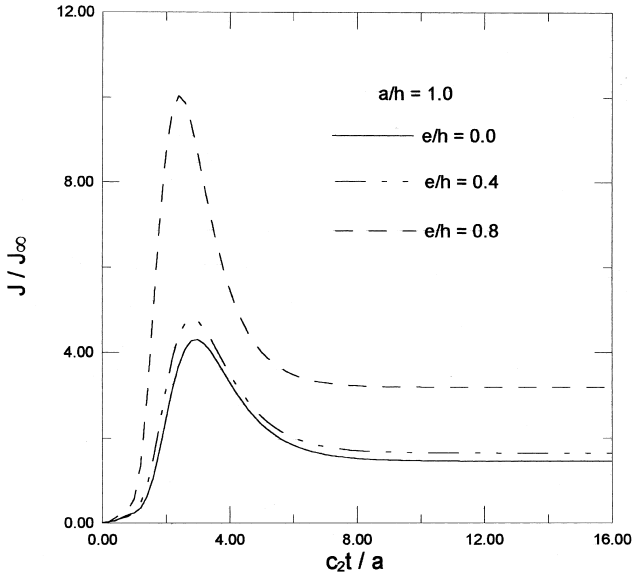

Fig. 5. Dynamic energy release rate of PZT-5H for various e/h values.

5. Conclusions

The electroelastic problem of an eccentric crack off the center line in a transversely isotropic piezoelectric ceramic strip under anti-plane impact shear was analyzed by the integral transform approach. The Fredholm integral equation is solved numerically. The traditional concept of linear elastic fracture mechanics is extended to include the piezoelectric effects and the results are expressed in terms of the dynamic stress intensity factor and the dynamic energy release rate. The dynamic energy release rates are dependent on the electric loading only under constant strain loading and independent of it under constant stress loading and always have positive values. The normalized dynamic stress intensity factor and energy release rate increase when the crack length and the eccentricity of crack location increase. The larger the crack length and eccentricity of crack location, the faster the time in arriving at peak values.

Acknowledgements

The authors are grateful for the supports provided by the Brain Korea 21 Project from the Korea Research Foundation (KRF) and a grant from the Korea Science and Engineering Foundation (KOSEF) and Safety and Structural Integrity Research Center at the Sungkyunkwan University.

References

Chen, Z.T., 1998. Crack tip field of an infinite piezoelectric strip under anti-plane impact. Mechanics Research Communications 25, 313–319.

Chen, Z.T., Yu, S.W., 1997. Anti-plane dynamic fracture mechanics in piezoelectric materials. International Journal of Fracture 85, L3–L12.

Khutoryansky, N.M., Sosa, H., 1995. Dynamic representation formulas and fundamental solutions for piezoelectricity. International Journal of Solids and Structures 32, 3307–3325.

Kwon, S.M., Lee, K.Y., 1999. Analysis of stress and electric fields in a rectangular piezoelectric body with a center crack under anti-plane shear loading. International Journal of Solids and Structures, in press.

Li, S., Mataga, P.A., 1996a. Dynamic crack propagation in piezoelectric materials – part I. electrode solution. Journal of the Mechanics and Physics of Solids 44 (11), 1799–1830.

Li, S., Mataga, P.A., 1996b. Dynamic crack propagation in piezoelectric materials – part II. vacuum solution. Journal of the Mechanics and Physics of Solids 44 (11), 1831–1866.

Miller, M.K., Guy, W.T., 1966. Numerical inversion of the Laplace transform by use of Jacobi polynomials. SIAM Journal on Numerical Analysis 3, 624–635.

Narita, F., Shindo, Y., 1998a. Dynamic anti-plane shear of a cracked piezoelectric ceramic. Theoretical and Applied Fracture Mechanics 29, 169–180.

Narita, F., Shindo, Y., 1998b. Scattering of Love waves by a surface-breaking crack in piezoelectric layered media. JSME International Journal Series A 41 (1), 40–48.

Pak, Y.E., 1990. Crack extension force in a piezoelectric materials. ASME Journal of Applied Mechanics 57, 647–653.

Paul, H.S., Nelson, V.K., 1996. Axisymmetric vibration of Piezo-composite hollow circular cylinder. Acta Mechanica 116, 213–222.

Shindo, Y., Ozawa, E., 1990. Dynamic analysis of a piezoelectric material. In: Hsieh, R.K.T. (Ed.), Mechanical Modeling of New Electromagnetic Materials. Elsevier, Amsterdam, pp. 297–304.

Shindo, Y., Katsura, H., Yan, W., 1996a. Dynamic stress intensity factor of a cracked dielectric medium in a uniform electric field. Acta Mechanica 117, 1–10.

Shindo, Y., Narita, F., Tanaka, K., 1996b. Electroelastic intensification near anti-plane shear crack in orthotropic piezoelectric ceramic strip. Theoretical and Applied Fracture Mechanics 25, 65–71.

Shindo, Y., Tanaka, K., Narita, F., 1997. Singular stress and electric fields of a piezoelectric ceramic strip with a finite crack under longitudinal shear. Acta Mechanica 120, 31–45.

Sneddon, I.N., 1972. The Use of Integral Transforms. McGraw-Hill, New York.